

## RESEARCH ARTICLE

# Epifluorescence, SEM, TEM and nanoSIMS image analysis of the cold phenotype of *Clostridium psychrophilum* at subzero temperatures

Amedea Perfumo<sup>1</sup>, Andreas Elsaesser<sup>2</sup>, Sten Littmann<sup>3</sup>, Rachel A. Foster<sup>3</sup>, Marcel M.M. Kuypers<sup>3</sup>, Charles S. Cockell<sup>4</sup> & Gerhard Kminek<sup>1</sup>

<sup>1</sup>European Space Agency, TEC-QI, Noordwijk, The Netherlands; <sup>2</sup>Leiden Institute of Chemistry, Leiden University, Leiden, The Netherlands; <sup>3</sup>Max Planck Institute for Marine Microbiology, Bremen, Germany; and <sup>4</sup>UK Centre for Astrobiology, School of Physics and Astronomy, University of Edinburgh, Edinburgh, UK

**Correspondence:** Amedea Perfumo, Helmholtz Centre Potsdam, GFZ German Research Centre for Geosciences, Telegrafenberg, D-14473 Potsdam, Germany. Tel.: +49 0 331 288 28755; Fax: +49 0 331 288 28802; e-mail: amedeia.perfumo@gfz-potsdam.de

**Present address:** Amedea Perfumo, Helmholtz Centre Potsdam, GFZ German Research Centre for Geosciences, Potsdam, Germany

**Present address:** Rachel A. Foster, Department of Ecology, Environment and Plant Sciences, Stockholm University, Stockholm, Sweden

Received 5 August 2014; revised 12 October 2014; accepted 12 October 2014. Final version published online 4 November 2014.

DOI: 10.1111/1574-6941.12443

Editor: Max Häggblom

## Keywords

cryo-adaptation; cell elongation; exopolysaccharide matrix; membrane vesicles; carbon storage granules.

## Introduction

Psychrophilic microorganisms inhabit cold environments where temperatures are usually near to or below 0 °C. They live not only in exotic habitats in the Arctic and Antarctic continents, for example, snow, glaciers, deep sea and sea ice, permafrost and caves (Margesin & Miteva, 2011), but also in domestic environments, for example refrigerators. Low temperatures pose serious threats to the preservation of cell functionality and viability, mainly due to an increase in water viscosity, decrease in molecular

## Abstract

We have applied an image-based approach combining epifluorescence microscopy, electron microscopy and nanoscale secondary ion mass spectrometry (nanoSIMS) with stable isotope probing to examine directly the characteristic cellular features involved in the expression of the cold phenotype in the Antarctic bacterium *Clostridium psychrophilum* exposed to a temperature range from +5 to −15 °C under anoxic conditions. We observed dramatic morphological changes depending on temperature. At temperatures below −10 °C, cell division was inhibited and consequently filamentous growth predominated. Bacterial cells appeared surrounded by a remarkably thick cell wall and a capsule formed of long exopolysaccharide fibres. Moreover, bacteria were entirely embedded within a dense extracellular matrix, suggesting a role both in cryo-protection and in the cycling of nutrients and genetic material. Strings of extracellular DNA, transient cell membrane permeability and release of membrane vesicles were observed that suggest that evolution via transfer of genetic material may be especially active under frozen conditions. While at −5 °C, the bacterial population was metabolically healthy, at temperatures below −10 °C, most cells showed no sign of active metabolism or the metabolic flux was extremely slowed down; instead of being consumed, carbon was accumulated and stored in intracellular granules as in preparation for a long-term survival.

diffusion rates, reduction in biochemical reaction rates and decrease in cell membrane fluidity, intracellular ice crystal formation and osmotic stress (Bakermans, 2008; Rodrigues & Tiedje, 2008). However, psychrophiles have developed a vast array of adaptive strategies on both cellular and molecular levels that have been identified by applying different experimental approaches and techniques. Besides the standard culturing and biochemical/biophysical analyses, ‘omic’ approaches are contributing to the discovery of many new aspects in cold adaptation (Casanueva *et al.*, 2010). Some recurrent characteristic

genes of the cold phenotype have been identified in the genome of psychrophiles, for example, genes for the transport of compatible solutes, the accumulation of carbon reserves, the use of alternative energy-efficient biosynthetic pathways, the synthesis of exopolysaccharides (EPS) and extracellular degradative enzymes (Méthé *et al.*, 2005; Riley *et al.*, 2008; Rodrigues *et al.*, 2008; Ayala-del-Río *et al.*, 2010; Collins & Deming, 2013; Mykytczuk *et al.*, 2013). Other analyses indicated that a cold transcriptome and cold proteome exist with most genes preferentially or uniquely expressed at low temperatures (Bakermans *et al.*, 2007; Rodrigues *et al.*, 2008; Bergholz *et al.*, 2009).

Microscopy-based techniques have been little used to observe the effect of low temperatures on microbial cells or to describe the phenotypic responses of microorganisms on a cellular level. Microscopy, however, has proved highly informative, especially if combined to fluorescent dye labelling (e.g. epifluorescence microscopy) or stable isotope probing (SIP) (e.g. nanoSIMS), and can provide important insights into the physiological and metabolic states of cells. In addition, electron microscopy-based imaging and analysis (scanning and transmission electron microscopy, SEM and TEM) enable us to study the compositional and structural features of microorganisms and their immediate surroundings at high resolution.

Numerous dyes are available that can be used with epifluorescence microscopy to provide information on viability of microorganisms and their physiological state (Müller & Nebe-von-Caron, 2010). Although some caveats must be considered when interpreting the data (e.g. cells stained 'red' with the LIVE/DEAD kit are not necessarily 'dead' but may be just 'stressed' with membranes temporarily injured), fluorescent labelling can be used to complement other imaging methods. For example, nanoscale secondary ion mass spectrometry (nanoSIMS) combined to SIP has been recently applied in microbiology studies. With nanoSIMS, after incubation with a labelled substrate, metabolic activity of single microbial cells can be imaged and the elemental composition can be measured on a subcellular level (Li *et al.*, 2008; Musat *et al.*, 2008; Wagner, 2008; Musat *et al.*, 2012; Pett-Ridge & Weber, 2012).

In this study, we have applied different imaging techniques – epifluorescence microscopy, SEM/TEM and stable isotope probing with nanoSIMS – in parallel and as complementary methods to investigate the cellular response and adaptation to subzero temperatures in the Antarctic bacterium *Clostridium psychrophilum*.

*Clostridium psychrophilum* DSM 14207 is an obligate psychrophilic anaerobic bacterium isolated from a microbial mat collected at Lake Fryxell, a permanently ice-covered lake located in the McMurdo Dry Valleys, Antarctica

(Brambilla *et al.*, 2001). *Clostridium psychrophilum*, as an extremophilic organism, is of considerable importance to assess the potential for cold-adapted terrestrial microbial forms to survive and perhaps proliferate on icy planets of our solar system (e.g. Mars) that will be the target of the upcoming life detection missions (e.g. ExoMars 2018, Mars 2020). *Clostridium psychrophilum* was selected as model organism for this study given the earlier description by Spring *et al.* (2003) as the most psychrophilic of the all known clostridia, with an optimum growth temperature  $T_{\text{opt}} = +4\text{ }^{\circ}\text{C}$  and an upper limit  $T_{\text{max}} = +10\text{ }^{\circ}\text{C}$ . Here, we provide direct observations of the bacterium's structure/ultrastructure and related physiological state at temperatures that extend down to  $-15\text{ }^{\circ}\text{C}$ . Our findings highlight the ecological role of some features distinctive to psychrophily such as temperature-dependent morphological variability and cryo-protection inferred by cell wall-thickening, EPS capsule and extracellular matrix production. Observations of extracellular DNA (eDNA) and release of membrane vesicles (MVs) and evidence for transient cell membrane permeability are also presented and discussed.

## Materials and methods

### Bacterial strain and cultivation conditions

The bacterial strain used in this study is *C. psychrophilum* DSM 14207, obtained from the Deutsche Sammlung von Mikroorganismen und Zellkulturen (DSMZ)-German Collection of Microorganisms and Cell Cultures. It was cultivated on the recommended liquid medium DSM 339 (Wilkins-Chalgren anaerobe broth supplemented with 0.5% w/v glucose and 0.1% w/v  $\text{NaHCO}_3$ ) and gas atmosphere consisting of 80%  $\text{N}_2$  and 20%  $\text{CO}_2$  and incubated at temperatures of  $+5$ ,  $-5$ ,  $-10$  and  $-15\text{ }^{\circ}\text{C}$ . To prevent freezing, the medium for incubation at subzero temperatures was supplemented with 5% (v/v) glycerol. To avoid thermal shock, culture bottles were kept on ice during handling. Reagents, medium and needles were chilled before use. Incubation was continued for c. 2–3 weeks at  $+5\text{ }^{\circ}\text{C}$  and for 5–6 weeks at  $-5\text{ }^{\circ}\text{C}$  before turbidity in the culture could be observed. Cells were harvested during the exponential phase when cell density reached  $1.5 \pm 0.5 \times 10^9\text{ cells mL}^{-1}$  (after 18 days) at  $+5\text{ }^{\circ}\text{C}$ , and  $7.0 \pm 2.0 \times 10^8\text{ cells mL}^{-1}$  (after 40 days) at  $-5\text{ }^{\circ}\text{C}$ . Cultures at  $-10$  and  $-15\text{ }^{\circ}\text{C}$  were kept incubated for almost 1 year without visible signs of growth.

### Epifluorescence microscopy

Cell staining using SYBR Green I (Molecular Probes, Invitrogen, CA) was performed according to Patel *et al.*

(2007) and cell staining with LIVE/DEAD BacLight (Molecular Probes, Invitrogen) following manufacturer's instructions. Stained cells were observed with a Leica Aristoplan epifluorescence microscope (Leica, Bensheim, Germany) equipped with a mercury lamp and fitted with filter cubes L3 (excitation BP 450–490, dichromatic mirror 510 nm and suppression LP 515) and N2.1 (excitation BP 515–560, dichromatic mirror 580 nm and suppression LP 590).

## Electron microscopy

### Fixation with formaldehyde–glutaraldehyde

Bacterial cells were harvested for electron microscopy analysis during the exponential phase, after 16-day incubation at +5 °C and 40-day incubation at –5 °C, or after 7-month incubation at –10 and –15 °C. Samples of the bacterial cell cultures were filtered onto a black polycarbonate Nuclepore membrane filter (pore size 0.22 µm; diameter 25 mm) and washed with Milli-Q water. The filter was placed into a petri dish, fixed for 1 h at +5 °C with a fixative solution containing 5% (v/v) formaldehyde and 2% (v/v) glutaraldehyde in cacodylate buffer (0.1 M cacodylate, 0.09 M sucrose, 0.01 M CaCl<sub>2</sub>, 0.01 M MgCl<sub>2</sub>, pH 7.0) and then washed three times with cacodylate buffer.

### Fixation with lysine acetate–ruthenium red formaldehyde–glutaraldehyde

To visualise the capsular and extracellular material of the bacterium, we used the fixation technique reported by Hammerschmidt *et al.* (2005) with some modifications. Bacterial cell samples were filtrated onto a Nuclepore membrane as previously described. The filter was first fixed for 30 min on ice at +5 °C with 2% (v/v) formaldehyde, 2.5% (v/v) glutaraldehyde and 0.075 M lysine acetate, prepared in cacodylate buffer supplemented with 0.075% (w/v) ruthenium red. After washing with cacodylate buffer containing ruthenium red, the filter was fixed a second time for 3 h using the same fixative solution without lysine acetate. The filter was washed again three times with the same cacodylate–ruthenium red buffer.

### Scanning electron microscopy

The filters were dehydrated in a graded series of ethanol (10%, 30%, 50%, 70%, 90% and 100%) for 30 min each step, on ice at +5 °C, and overnight at 70% grade. After dehydration, they were let to air-dry. The filters were finally sputter-coated with a 12 nm thick gold film (Emitech K550X sputter coater; Quorum Technologies Ltd,

Ashford, UK) and observed with a Quanta FEG-650 SEM (FEI, Hillsboro, OR) operating at 5 kV and a working distance of 10 mm. In total, 71 micrographs were imaged at +5 °C, 55 at –5 °C, 93 at –10 °C and 83 at –15 °C.

### Transmission electron microscopy

Each filter was transferred to a clean petri dish, treated for 1 h with 1% (v/v) osmium tetroxide solution prepared in cacodylate buffer, or cacodylate–ruthenium red buffer for lysine acetate–ruthenium red (LRR)-fixed samples, and then washed three times in cacodylate buffer, or cacodylate–ruthenium red buffer, respectively. Samples were then dehydrated in ethanol gradients as described above and dried. Filters were embedded using LR White acrylic resin (medium grade; Electron Microscopy Sciences, Hatfield, PA) in a graded series of ethanol and resin (2 : 1, 1 : 1, 1 : 2), at 5 °C, in the dark, for 20 min each step, and finally transferred to 100% resin for 8 h, refreshed and incubated again overnight. Each filter was cut in small strips, and several of them were fit at the bottom of a gelatin capsule (size '0'; Electron Microscopy Sciences), which was then filled with pure resin. Air bubbles were removed in a vacuum oven (400 mbar, temp. 40 °C), and the resin was then left to polymerise at 55 °C for 48 h. Ultrathin sections (80 nm thick) were cut from polymerised resin blocks and mounted on 200-mesh copper grids. The grids were then poststained in 1% (v/v) uranyl acetate and Reynolds lead citrate, washed, air-dried and then viewed in a Philips CM120 transmission electron microscope operating at 80 kV. Representative images were taken with a Gatan Orius CCD camera. In total, 24 micrographs were imaged at +5 °C, 29 at –5 °C, 41 at –10 °C and 57 at –15 °C.

### Elemental imaging with nanoscale secondary ion mass spectrometry (nanoSIMS)

#### Sample preparation

*Clostridium psychrophilum* was cultivated as described previously on medium DSM 339 supplemented with <sup>13</sup>C-glucose (99%; Cambridge Isotope Laboratories, Andover, MA) at 0.5% (w/v) concentration. Cells incubated at –5 °C were sampled during the exponential phase (30 days), while cells incubated at –10 and –15 °C after 3 months. The culture was fixed by injecting 1% (v/v) chilled paraformaldehyde directly in the bottle and leaving incubated at 4 °C overnight. Cells were gently filtered onto a gold-palladium presputtered polycarbonate filter (pore size 0.22 µm; diameter 25 mm; Millipore), rinsed with sterile PBS and washed with sterile Milli-Q water to remove residues from the medium. The filter was air-

dried and stored at  $-20^{\circ}\text{C}$  until use. Subsamples were prepared by excising small circles (5 mm diameter) and stained with DAPI (Molecular Probes, Invitrogen), and the areas of interest were marked using a laser micro-dissection (LMD) microscope (LMD6500; Leica). Cells within the markings were first imaged with a Zeiss Axio-plan (Zeiss, Jena, Germany) epifluorescence microscope fitted with blue (450–490 nm) and green (510–560 nm) excitation filters, and then, filters were washed with Milli-Q water and ethanol to remove residues of oil and air-dried. These images were used for orientation during nanoSIMS analysis.

### Image acquisition

The nanoSIMS analysis was performed using a nanoSIMS 50-L (CAMECA, Paris, France) as previously described (Musat *et al.*, 2008). To implant caesium ( $\text{Cs}^+$ ), the sample surface was presputtered with a defocused  $\text{Cs}^+$  primary ion beam between 200 and 300 pA. The sample area ( $20\text{ }\mu\text{m} \times 20\text{ }\mu\text{m}$  or  $30\text{ }\mu\text{m} \times 30\text{ }\mu\text{m}$  depending on cell distribution) was then rastered with a 2 pA  $\text{Cs}^+$  primary ion beam with dwell time of 1 ms. Negative secondary ions  $^{12}\text{C}^-$ ,  $^{13}\text{C}^-$ ,  $^{12}\text{C}^{14}\text{N}^-$ ,  $^{12}\text{C}^{15}\text{N}^-$ ,  $^{31}\text{P}^-$  and  $^{32}\text{S}^-$  from each individual cell were collected simultaneously in electron multiplier detectors of the multi-collection system. In total, 215 single cells were imaged at  $-5^{\circ}\text{C}$ , 111 at  $-10^{\circ}\text{C}$  and 124 at  $-15^{\circ}\text{C}$ .

### Image and data processing

Image and data analysis was performed using Look@NanoSIMS software (Polerecky *et al.*, 2012). For each image, all scans (50 planes) were corrected for drift of the sample stage during image acquisition and accumulated. Regions of interest were manually drawn around single cells, and the ratios  $^{13}\text{C}/^{12}\text{C}$  were calculated from the accumulated data. The  $^{31}\text{P}^-$ ,  $^{12}\text{C}^{14}\text{N}^-$  and  $^{32}\text{S}^-$  ion images were normalised to  $^{12}\text{C}$  to remove possible tuning effects.

### Cell surface area and volume calculations

Cell dimensions (length,  $l$ , and width,  $w$ ) were determined on the cells imaged with the scanning electron microscope using the open source image processing program IMAGEJ 1.48 (freely available at <http://imagej.nih.gov/ij/index.html>). Bacteria were assumed shaped like cylinders with hemispherical ends; therefore, the surface area ( $S$ ) and the volume ( $V$ ) were calculated according to Baldwin & Bankston (1988) as:

$$S = 4\pi(w/2)^2 + 2\pi(w/2)(l - w)$$

$$V = 4\pi(w/2)^3/3 + \pi(w/2)^2(l - w)$$

with  $w$  = cell width (i.e. cell diameter) and  $l$  = cell length.

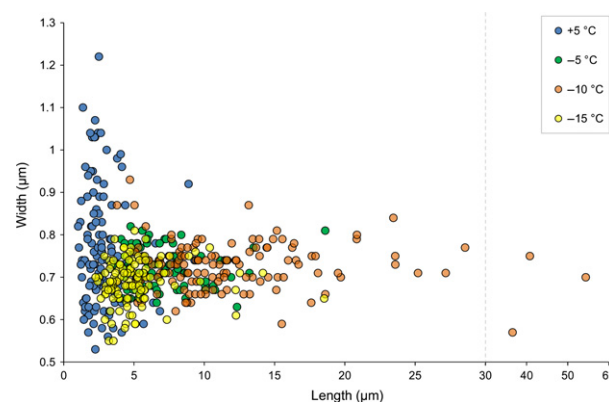
### Statistical analysis

One-way analysis of variance (ANOVA) was used to assess differences in cell dimensions (length, width, surface area and volume) and their ratios at the different incubation temperatures ( $+5$ ,  $-5$ ,  $-10$  and  $-15^{\circ}\text{C}$ ). Means comparison was evaluated by the Bonferroni test. Significance was calculated at the 1% and 5% level.

## Results and discussion

### Temperature-dependent morphological changes in *C. psychrophilum* cells





Cells of *C. psychrophilum* incubated at a temperature range from  $+5$  to  $-15^{\circ}\text{C}$  showed a high level of morphological variation. In general, we observed that cells were gradually longer at lower temperatures down to  $-10^{\circ}\text{C}$ , as shown by an increased length-to-width ratio ( $l/w$ ), while at  $-15^{\circ}\text{C}$ , cells restored shorter dimensions (Fig. 1 and Supporting Information, Fig. S1, Table 1). The analysis of variance (ANOVA) test supported, at a high level of significance (at the 0.01 level), that decreasing subzero temperatures have a strong effect on cell size and morphology. At  $+5^{\circ}\text{C}$ , cells appeared highly pleomorphic, with irregular shapes and many coccoid-like forms. At  $-5^{\circ}\text{C}$ , the bacterium was rod shaped ( $4.0$ – $10.0\text{ }\mu\text{m}$  length  $\times$   $0.65$ – $0.80\text{ }\mu\text{m}$  width). At  $-10^{\circ}\text{C}$ , cells appeared elongated ( $4.00$ – $20.00\text{ }\mu\text{m}$  length  $\times$   $0.65$ – $0.80\text{ }\mu\text{m}$  width)



**Fig. 1.** Size variability of *Clostridium psychrophilum* cells incubated anaerobically at temperatures from  $+5$  to  $-15^{\circ}\text{C}$  measured by SEM (dotted line indicates scale change).



**Table 1.** Overview of the morphological features of cells of *Clostridium psychrophilum* incubated at temperatures from +5 to −15 °C observed with scanning electron microscopy (SEM) and processed with IMAGEJ program

Temp. (°C)	No. of cells measured	Length (l) and width (w) (μm) average [SD]	l/w ratio [SD]	Cell morphology	Surface area (S) (μm <sup>2</sup> ) average [SD]	Volume (V) (μm <sup>3</sup> ) average [SD]	S/V ratio [SD]
+5 <sup>†</sup>	114	2.74** [1.40] × 0.77** [0.14]	3.69** [2.05]		6.60** [3.50]	1.17* [0.76]	6.02 <sup>(*)</sup> [0.92]
−5 <sup>†</sup>	86	7.24** [2.65] × 0.72 <sup>(*)</sup> [0.05]	10.07* [3.70]		16.42** [6.21]	2.88** [1.20]	5.77 <sup>(*)</sup> [0.36]
−10 <sup>†</sup>	125	12.22** [7.13] × 0.73 <sup>(*)</sup> [0.06]	16.95** [10.30]		27.84** [16.09]	4.98** [2.98]	5.67 <sup>(*)</sup> [0.42]
−15 <sup>‡</sup>	123	5.09** [2.39] × 0.69* [0.05]	7.40* [3.53]		11.06** [5.24]	1.83* [0.94]	6.15 <sup>(*)</sup> [0.47]

\*Means are significantly different to all other means at the 0.05 level (ANOVA–Bonferroni). \*\*Means are significantly different to all other means at the 0.01 level (ANOVA–Bonferroni); if in brackets means are significantly different to some but not to all other means.

<sup>†</sup>Liquid culture medium.

<sup>‡</sup>Frozen culture medium.

and in some cases filamentous, some of which measured up to 55 μm in length (Fig. 2). At −15 °C, cells appeared as rods 5.09 ± 2.39 μm long and 0.69 ± 0.05 μm wide. As general trend, we observed that, in response to gradu-

ally lower temperatures down to −10 °C, cells increased significantly (ANOVA–Bonferroni at the 0.01 level) their total surface area without any appreciable increase in the surface-to-volume ratio (ANOVA–Bonferroni at the 0.05

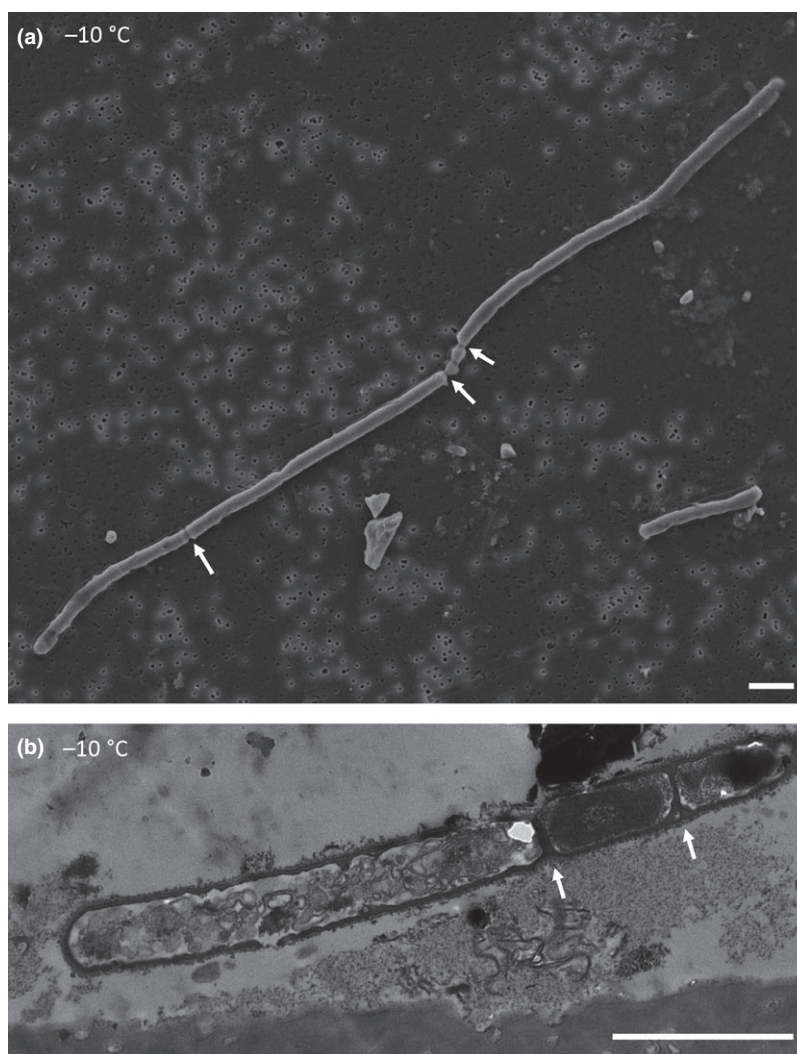


**Fig. 2.** Filamentous growth of cells of *Clostridium psychrophilum* at −10 °C imaged with SEM (a) and TEM (b). Filaments up to 50 μm length were observed. Septa (indicated by arrows) were visible throughout the filament in the micrograph by SEM (a), and TEM confirmed the ultrastructure of new membranes forming between the cells (b). Interestingly, individual cells did not separate, indicative of an interruption of the cell division. Scale bar represents 2 μm.

level limited to a few means only; Table 1). This phenomenon has been described previously in microorganisms exposed to various stress conditions and especially under nutrient deprivation (Young, 2006). Our data indicate that in supercooled liquid media, where the diffusion rate of molecules is sensibly reduced by the temperature, bacterial cells with enlarged surface have the advantage of a more efficient access to nutrients. At  $-15^{\circ}\text{C}$ , under frozen conditions, cells showed an opposite trend, with still an increase in length (at the 0.01 level) compared to positive temperatures but decrease in width (at the 0.05 level). Differently to the bacteria in supercooled media, the surface-to-volume ratio of cells at  $-15^{\circ}\text{C}$  was significantly (0.01 level) increased.

Salts such as NaCl and  $\text{Mg}(\text{ClO}_4)_2$  were also tested as additional freezing depression additives to maintain liquid conditions also at  $-15^{\circ}\text{C}$ , but the culture did not grow. In fact, as isolated from a freshwater lake (Lake Fryxell, Antarctica), *C. psychrophilum* does not tolerate high salinity. This might reduce its growth potential at subzero temperatures compared to other bacteria such as *Planococcus halocryophilus* (Mykytczuk *et al.*, 2013) and *Psychrobacter cryopagella* (Bakermans *et al.*, 2003) capable of reproducing at  $-15$  and  $-10^{\circ}\text{C}$ , respectively, at higher rates. On the other hand, *C. psychrophilum* is a strictly anaerobic organism that offers the rare possibility to study subzero growth in environments devoid of oxygen.

That bacteria can alter their size and shape in response to changes in the environmental conditions or to stress factors is well known. Filamentation is one of the most frequently observed shape alterations and can be triggered by various factors, for example, nutrient deprivation, oxidative stress, DNA damage and antibiotics exposure (Young, 2006; Justice *et al.*, 2008). Filamentous cells were also described in bacteria, including other clostridia, growing at suboptimal temperatures or temperatures near the minimum for growth (Marchant *et al.*, 2002; de Jong *et al.*, 2004; Abboud *et al.*, 2005; Jones *et al.*, 2013). Although the exact molecular mechanisms leading to filamentation are largely unknown, some have shown that it is a consequence of blocking the late stages of the cell division while the cell continues to grow (Burke *et al.*, 2013). When *C. psychrophilum* cells were stained with DNA-specific SYBR Green I, we could observe that nucleoids were present and evenly spaced throughout the filaments (Fig. S1). With electron microscopy, indentations were at times also visible, and some septa appeared complete with new membranes formed between the daughter cells; however, cells remained connected within the filament (Fig. 2). Our latter observations support a disruption of the spatial and temporal distribution of the cell division machinery under stress conditions. It has been suggested that filamentation may be linked to a

reduced energy state (Jones *et al.*, 2006) as, for example, caused by subzero temperatures. In contrast to the perception of filamentous bacteria as over-stressed and dying, recent studies on several different organisms have in fact associated the filamentous phenotype with a survival strategy in various situations, for example, tolerance of stress factors (Crabbé *et al.*, 2012; Jones *et al.*, 2013), biofilm formation (Yoon *et al.*, 2011), protection from predation (Swanson, 2013) and resistance to antibiotics (Justice *et al.*, 2008). Additionally, it has been shown that filamentous cells can develop cross-protection over multiple stresses at sublethal levels (reviewed in Justice *et al.*, 2008 and Jones *et al.*, 2013). Although we did not observe it to occur in our experiments, it has also been reported that the filamentous state may be reversible and that, when cells return to more favourable conditions, the capacity to divide is restored (Jones *et al.*, 2013).

### Bacterial cell surface, EPS and extracellular matrix

To observe the bacterial cell surface and its constituents and structure, we used electron microscopy (SEM and TEM) and a fixation method that combines lysine acetate and ruthenium red (LRR fixation) for an enhanced preservation and visualisation of the cell capsular material (Hammerschmidt *et al.*, 2005). Conventional glutaraldehyde–formaldehyde fixation resulted in the total loss of capsular material, while extracellular features were clearly visible in the LRR-treated samples (Fig. S2). Therefore, we could observe that at all temperatures, the bacteria were coated with a capsule, loose-knit branched and composed of two distinct layers of exopolysaccharide (EPS) material. The EPS was compact with an electron-dense inner layer (25 nm thick as measured on the TEM image) and a fibrous outer layer. In some cells, at  $-15^{\circ}\text{C}$ , such EPS fibres protruded from the cell wall for about 100 nm (Fig. 3).

In pathogenic clostridia, the presence of the capsule is associated with virulence, in that it aids cell adhesion to surfaces and confers resistance to antibiotics (Brook, 1986). Given our consistent observation of a thick protruded EPS in the *C. psychrophilum* grown at subzero temperatures, the EPS capsular material is likely to have an important role in cryo-protection. A few genomes of psychrophiles, for example, *Psychrobacter* spp., *Colwellia psychrerythraea* H34 and *Exiguobacterium sibiricum*, have been found to possess genes involved in the synthesis of capsular-type EPS and express these genes at subzero temperatures ( $-2.5^{\circ}\text{C}$ ) (Méthé *et al.*, 2005; Rodrigues *et al.*, 2008; Allen *et al.*, 2009; Ayala-del-Río *et al.*, 2010). Large amounts of free EPS have also been found in sea ice and released by the indigenous organisms (Krembs

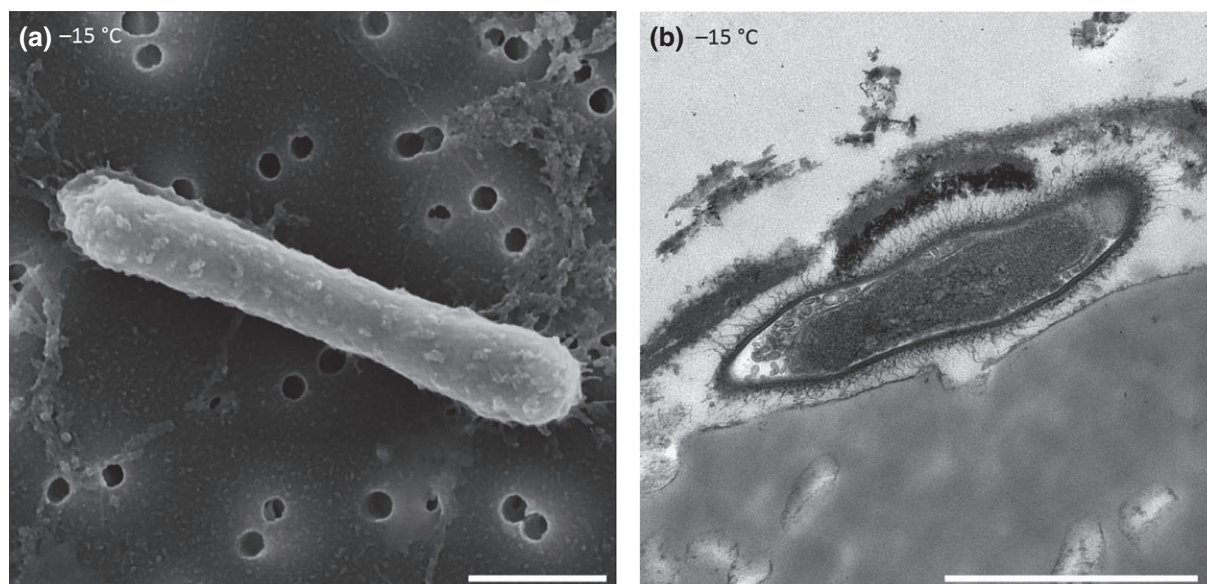


**Fig. 3.** Capsular structure of *Clostridium psychrophilum* visualised with SEM (a) and TEM (b) in LRR-fixed cells. Prior to imaging, bacteria were kept incubated in frozen media at  $-15^{\circ}\text{C}$  for 7 months. Scale bar represents  $1\text{ }\mu\text{m}$ .

*et al.*, 2011). Considering the data available in the literature, the ecological significance of EPS seems twofold: first, in protecting the cells from environmental fluctuations, and second, in altering conditions favourably in the surrounding environment (Krembs & Deming, 2008). Cell–EPS aggregates have been reported to act as colonisation points for microorganisms in sea ice, thus forming ‘hot spots’ of enhanced microbial activity (Meiners *et al.*, 2008). In its natural environment, *C. psychrophilum* was isolated from a microbial mat inhabited by a rich microbial community, and in the laboratory it also tends to grow planktonically forming aggregates.

SEM observations also revealed that cells of *C. psychrophilum* at  $-10^{\circ}\text{C}$  were encased within a thick extracellular matrix (Fig. 4a and b). The extracellular matrix was also composed of dead cellular material and fragments of cellular membranes. The nanoSIMS imaging indicated that the extracellular matrix was rich in fundamental elements, that is carbon and nitrogen (Fig. 4c), and also contained localised areas (nm) of sulphur (Fig. 4d). The possibility that the sulphur accumulation originates from the medium or the fixatives cannot be ruled out. However, although all samples have been processed in the same way, hot spots of sulphur were seen only in the  $-10^{\circ}\text{C}$  culture. Sulphur may be of biological origin and be contained in hydrogen sulphide, carbon disulphide and other sulphur compounds that are known metabolic products of clostridia (Kuppusami *et al.*, 2014).

Moreover, when epifluorescence microscopy was used in combination with the nucleic acid-specific probe

SYBR Green I, strands of extracellular DNA (eDNA) were observed crossing and connecting the cells’ matrix into aggregates (Fig. 5). Similar images of eDNA stained with nucleic acid-specific SYTO9 dye are also presented in Flemming & Wingender (2010). For a long time, eDNA was considered just as residual material from lysed cells, but it has become increasingly clear that, in fact, it is an integral part of the biofilm matrix and has an active role in many processes including bacterial adhesion and aggregation onto surfaces, scaffolding and strengthening, exchange of genetic information and finally as a source of nutrient and intermediates in the phosphorus cycling (Das *et al.*, 2010; Flemming & Wingender, 2010; Gloag *et al.*, 2013). Only a few psychrophilic organisms, for example, *Psychromonas arctica* (Groudieva *et al.*, 2003), *Psychrobacter arcticus* (Hinsa-Leasure *et al.*, 2013) and *Thiomicrospira* species (Niederberger *et al.*, 2009) have been described so far as capable of producing biofilms at low temperatures ( $4^{\circ}\text{C}$ ). In frozen environments, ‘biofilms’ may help bacterial cells to attach onto the surface of soil minerals and organic particles and gain access to the surrounding thin film of liquid water (Clarke *et al.*, 2010; Hinsa-Leasure *et al.*, 2013). Moreover, biofilms are particularly important in perennially cold habitats to facilitate lateral gene transfer as such to compensate for the very low rates of generation time of the indigenous organisms as demonstrated to occur for the haloarchaea populating an isolated Antarctic lake (DeMaere *et al.*, 2013). In such context, research should continue to identify the role of gene



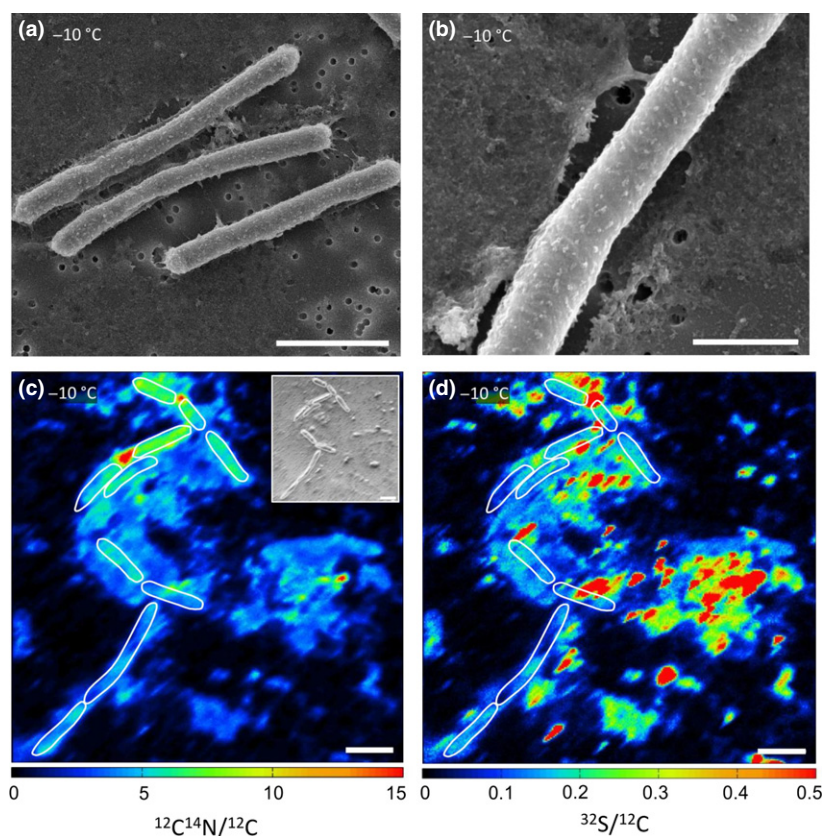


**Fig. 4.** Extracellular matrix produced by *Clostridium psychrophilum* at  $-10\text{ }^{\circ}\text{C}$ . As shown in the SEM micrographs (a, b), cells appeared completely embedded in a thick ( $1.3\text{--}1.5\text{ }\mu\text{m}$ ) extracellular matrix. The nanoSIMS imaging showed that the matrix between the cells is rich in carbon and nitrogen ( $^{12}\text{C}^{14}\text{N}/^{12}\text{C}$ ) (c) and has localised 'hot spots' of sulphur  $^{32}\text{S}/^{12}\text{C}$  (d). White outlines in the nanoSIMS images show regions of interest and cellular boundaries of *C. psychrophilum*. Inset in (c) is the respective secondary electron image. Cells were not clearly visible because covered by the extracellular matrix. Scale bar represents  $3\text{ }\mu\text{m}$ .

transfer vs. DNA replication in the acquisition of cold-adaptive traits and the overall microbial evolution in frozen habitats.

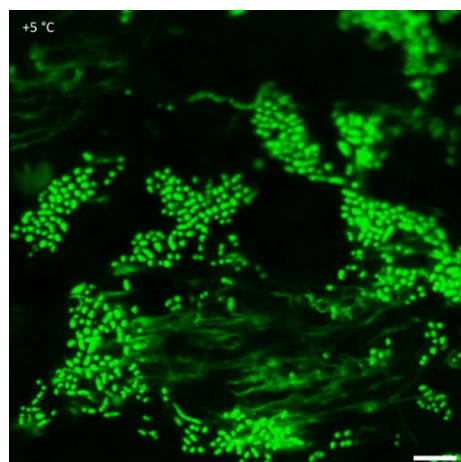


**Fig. 5.** Extracellular DNA (eDNA) in *Clostridium psychrophilum* culture stained with nucleic acid-specific dye SYBR Green I and imaged with epifluorescence microscopy ( $\times 50$ ). Strands of eDNA appeared to cross and connect aggregates of cells. Culture was grown at  $+5\text{ }^{\circ}\text{C}$ . Scale bar represents  $10\text{ }\mu\text{m}$ .

### Ultrastructure of *C. psychrophilum* at subzero temperatures

The ultrastructure is a largely unexplored aspect of the physiology of psychrophilic microorganisms, and only a few studies have been carried out until now on bacteria exposed to subzero temperatures (Bakermans *et al.*, 2003; Pecheritsyna *et al.*, 2011; Mykytchuk *et al.*, 2013). Part of the reason is the very low cell numbers that can be obtained under such conditions. We tried to overcome this problem by concentrating the biomass onto a membrane filter, which would still be compatible with the ultra-thin sectioning process required for TEM sample preparation.

At all subzero temperatures, cells of *C. psychrophilum* were characterised by a very thick cell wall measuring up to  $50\text{ nm}$  (Fig. 6). A similar feature was also observed in permafrost isolates at temperatures of  $0\text{--}4\text{ }^{\circ}\text{C}$  (Soina *et al.*, 1995). The thickening of the cell wall may well represent a general protection mechanism amongst cold-adapted microorganisms against freezing and osmotic stress.

In addition, while the cell membrane of cells incubated at  $-5\text{ }^{\circ}\text{C}$  appeared to be contiguous to the cell wall, at the lower temperatures, gaps between wall and membrane



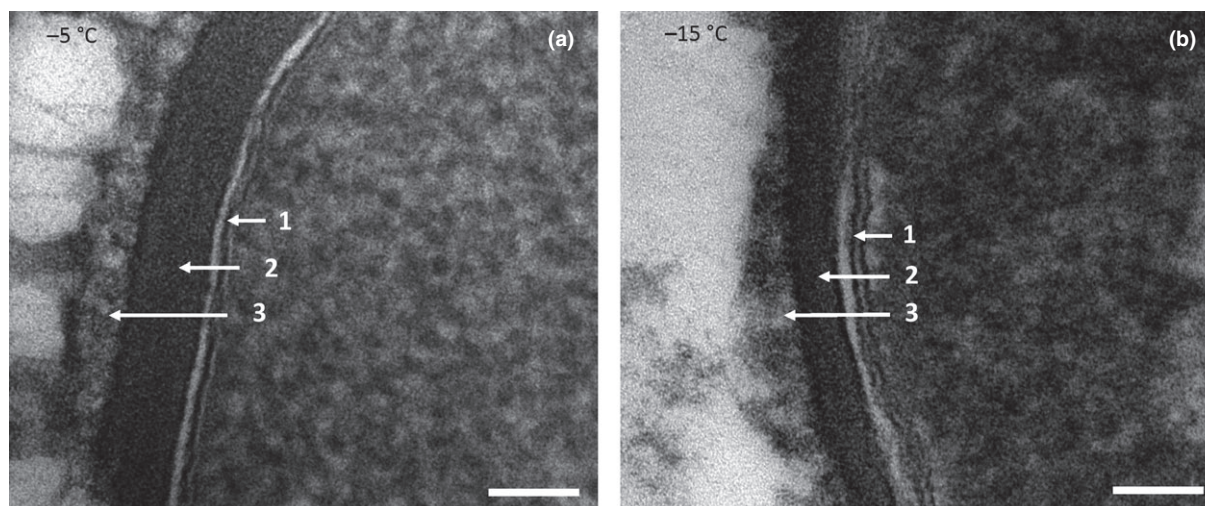


**Fig. 6.** Ultrastructure observed by TEM of the cell envelope of cells of *Clostridium psychrophilum* at  $-5^{\circ}\text{C}$  (a) and  $-15^{\circ}\text{C}$  (b). Three regions can be clearly distinguished: the cell membrane (1), the thick (c. 50 nm) cell wall (2) and the outer fibrous layer representing the extracellular capsule (3). Cell wall and membrane appear as contiguous in cells at  $-5^{\circ}\text{C}$  (a), but partially detached in cells at  $-15^{\circ}\text{C}$  (b). Scale bar represents 50 nm.

were visible (Fig. 6). These related to the cell plasmolysis, a consequence of the freezing of the environment surrounding the cells. When the freezing rates are low, the formation of extracellular ice induces high solute concentration in the medium and water is consequently drawn out of the cytoplasm, which results in the cell deflating and space to form between wall and membrane (Mazur, 1984; Schwarz & Koch, 1995; Fonseca *et al.*, 2006). We observed plasmolysed cells in higher number (c. 20% of the overall population, i.e. 40/160 cells observed at  $-10^{\circ}\text{C}$  and 40/200 cells at  $-15^{\circ}\text{C}$ ) at the lowest incubation temperatures and frozen media (Fig. 7), while they were absent at  $-5^{\circ}\text{C}$  when the medium was still liquid. Plasmolysis is considered a physiological state mostly associated with cell damage and death as here substantiated by the presence of red-stained cells in the LIVE/DEAD analysis at temperatures below  $-10^{\circ}\text{C}$ .

Moreover, during plasmolysis, the shrinkage of the protoplast results in a considerable reduction of the total area of the cell membrane and a fraction of it excises in the form of MVs (Matias & Beveridge, 2005). We also observed pockets filled with MVs consistently in the plasmolysed cells (Fig. 7). The release of vesicles from the cell surface is a phenomenon conserved across microbial life, and it has been described in both Gram-negative and Gram-positive bacteria, archaea and eukaryotes (Deatherage & Cookson, 2012). The composition of the MVs from various species has been characterised by SDS-PAGE and proteomics (Kulp & Kuehn, 2010), and results showed that they consist of proteins, lipoproteins, phospholipids and lipopolysaccharides derived from the cell surface and

contain cytoplasmic proteins (Frias *et al.*, 2010) and also genomic and plasmid DNA (Gaudin *et al.*, 2013). MVs have also been observed and described as a common feature in cold-adapted Antarctic organisms such as *Shewanella livingstonensis* NF22, *Shewanella vesiculosa* M7, *Pseudoalteromonas* sp. M4.2 and *Psychrobacter fozii* NF23 (Frias *et al.*, 2010). Several roles, mainly related to stress-response and survival, have been attributed to the MVs, including relieving the cell surface from misfolded or damaged material, nutrient acquisition, mediating communication amongst cells, and both secretion and transfer of DNA (Kulp & Kuehn, 2010).

### Physiological state of *C. psychrophilum* in frozen conditions

The physiological state of a bacterial cell depends largely on the integrity of the cell membrane and whether it is permeable for nutrients from the surroundings. When we stained the cells of *C. psychrophilum* incubated at  $-5^{\circ}\text{C}$  with propidium iodide (PI), we found that the majority of cells was not permeable to PI but were counterstained green with SYTO9, thus indicating that cell membrane was intact and functional (Fig. 8a). This was consistent with the nanoSIMS images that showed high isotopic intracellular enrichment of  $^{13}\text{C}/^{12}\text{C}$ , which indicated that the  $^{13}\text{C}$ -glucose, used by the bacterium as carbon source, was taken up and incorporated into the cell (Fig. 8b). Thus,  $-5^{\circ}\text{C}$  is clearly a temperature still favourable for *C. psychrophilum* to maintain a healthy and growing cell population. At lower temperatures,  $-10^{\circ}\text{C}$  and  $-15^{\circ}\text{C}$ ,

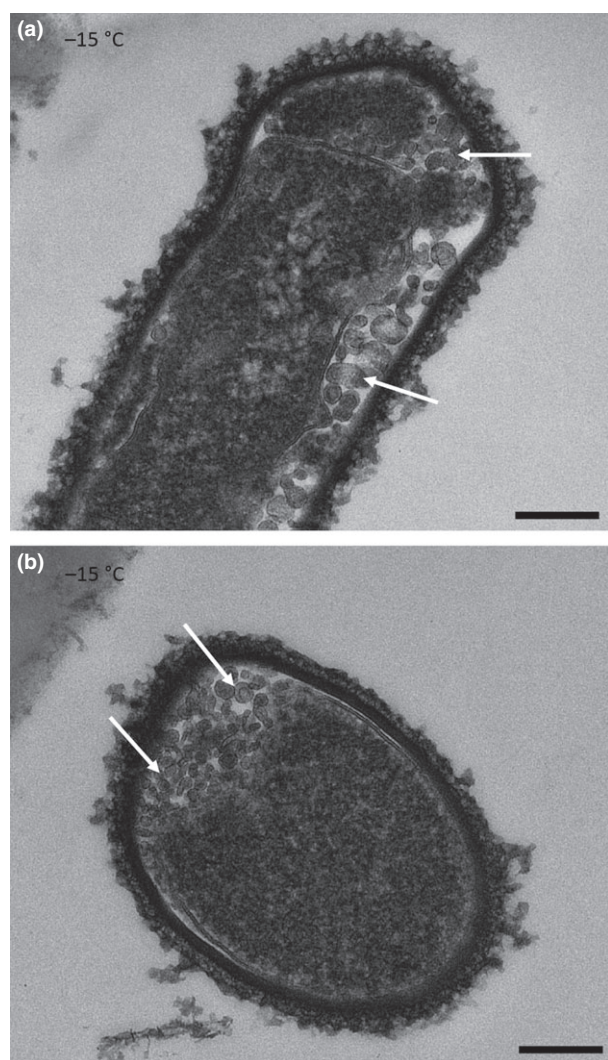


**Fig. 7.** Plasmolysed cells of *Clostridium psychrophilum* at temperatures of  $-15\text{ }^{\circ}\text{C}$  imaged by TEM. The periplasmic space appears filled with membrane vesicles (indicated by arrows) formed by the membrane contraction consequent to the freezing-induced osmotic stress. Cells are shown thin-sectioned longitudinally (a) and transversely (b). Scale bar represents 200 nm.

however, most cells fluoresced red, indicating that the membrane was permeable allowing PI to pass through. In addition, we noted that in some cells, the red PI stain was not evenly distributed, but interspersed between areas staining green (Fig. 8c). The latter suggests that the membrane was either locally or temporarily permeable to PI. Similar observations were made by Suo *et al.* (2009), and Davey & Hexley (2011) when studying *Salmonella typhimurium* and *Saccharomyces cerevisiae* exposed to physical (mechanical puncturing and heat treatment) and chemical (ethanol exposure) stress. Moreover, Davey & Hexley (2011) suggested an interesting possible evolution-

ary implication for the transient membrane permeability as a way to facilitate horizontal gene transfer.

NanoSIMS imaging also showed no or extremely low  $^{13}\text{C}$ -isotopic enrichment for a higher percentage of the cells incubated at  $-10$  and  $-15\text{ }^{\circ}\text{C}$  (Fig. 8d). This indicated that, at these lower temperatures, most cells were metabolically inactive (with respect to glucose) or that the metabolic rates were very low and hardly detectable.

It was interesting to observe with TEM that bacterial cells incubated especially at subzero temperatures,  $-10$  and  $-15\text{ }^{\circ}\text{C}$ , accumulated large quantities of intracellular granules (Fig. 9). The intracellular accumulation of polysaccharide-containing granules as a cold adaptation strategy has been reported for *Clostridium algariphilum* (Pecheritsyna *et al.*, 2011) and a few other psychrophilic organisms (Jeon *et al.*, 2004). Genes involved in the synthesis of glucose polymers such as polyhydroxyalkanoates and glucans were also detected in the genomes of psychrophiles *Colwellia psychrerythraea* 34H and *Exiguobacterium sibiricum*, respectively (Methé *et al.*, 2005; Rodrigues *et al.*, 2008). Similar to our observations here on *C. psychrophilum*, the storage of carbon polymers also increased in *C. algariphilum* with decreasing temperatures and was highest at  $-5\text{ }^{\circ}\text{C}$  (23% of the total biomass content) (Pecheritsyna *et al.*, 2011).

These inclusion bodies are likely to act as compatible solutes that protect against freezing and osmotic effects. Moreover, it is also possible that, under limiting thermal stress conditions for cell proliferation, the available carbon is used by the cells as storage, which can be interpreted as the initial step in preparation to a long-term survival of microorganisms in cryo-environments. Carbon-based polymers are degraded slowly, and the slower this occurs, the longer the bacterium can survive. This suggests that alternatives exist in clostridia, besides the capability to form spores, to withstand temperature extremes.

## Acknowledgements

We thank R. Lindner and A. Dowson for the support received throughout the project at the Life Support (LIS) Laboratory at ESA/ESTEC. We also thank S. Mitchell for technical assistance with the TEM, R. Pukall for advice with regard to strain handling, D. Franzke and D. Nini for the support with the nanoSIMS analysis and R. Marchant for valuable comments on the manuscript. A.P. was supported by the Research Fellowship programme of the European Space Agency. R.A.F. is supported by the Knut and Alice Wallenberg Foundation. The TEM work was sponsored by the Science and Technology Facilities Council (STFC), Grant No. ST/1001964/1, and the nanoSIMS analyses by the Max Planck Society.



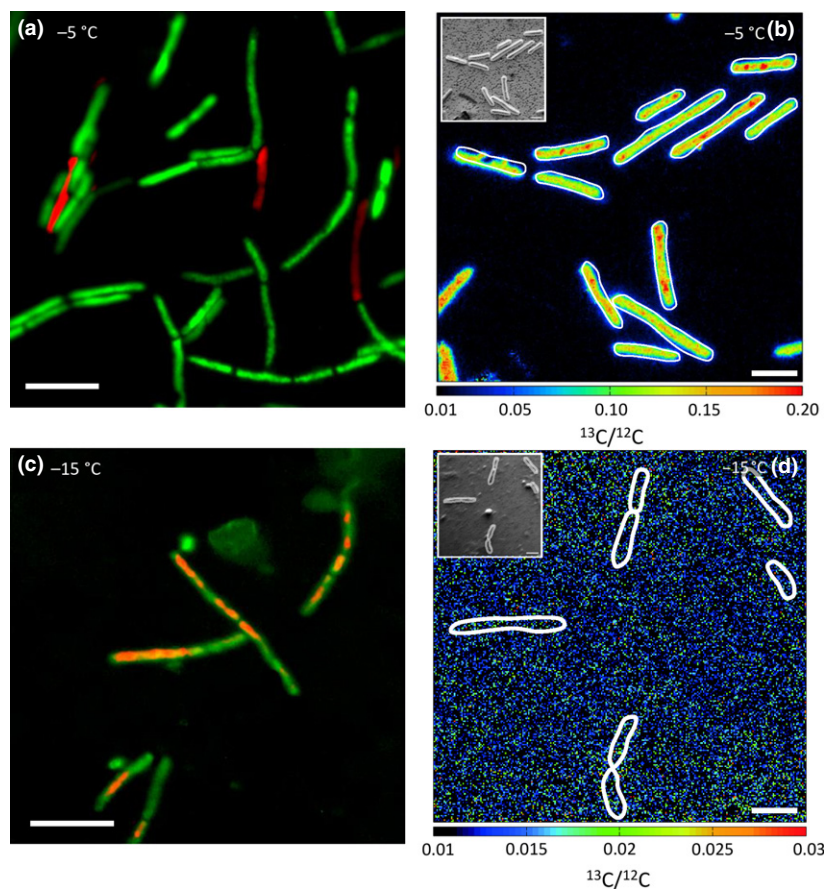


**Fig. 8.** Comparison of physiological state and elemental composition of bacterial cells incubated with  $^{13}\text{C}$ -glucose at  $-5$  and  $-15$  °C inferred by LIVE/DEAD staining and the  $^{13}\text{C}/^{12}\text{C}$  ratio image by nanoSIMS. Healthy cells at  $-5$  °C fluoresce green (a) and have a high intracellular  $^{13}\text{C}/^{12}\text{C}$  (b). Instead, at  $-15$  °C, cells fluoresce unevenly red and green (c) possibly due to localised/transient membrane damage, and their internal isotopic enrichment is very low and close to the natural abundance (d). The white lines in the nanoSIMS images define the regions of interest that were used to calculate the  $^{13}\text{C}/^{12}\text{C}$  ratios. Insets (b) and (d) are the respective secondary electron images. Scale bar in (a) and (c) represents 5 μm, and scale bar in (b) and (d) represents 3 μm.

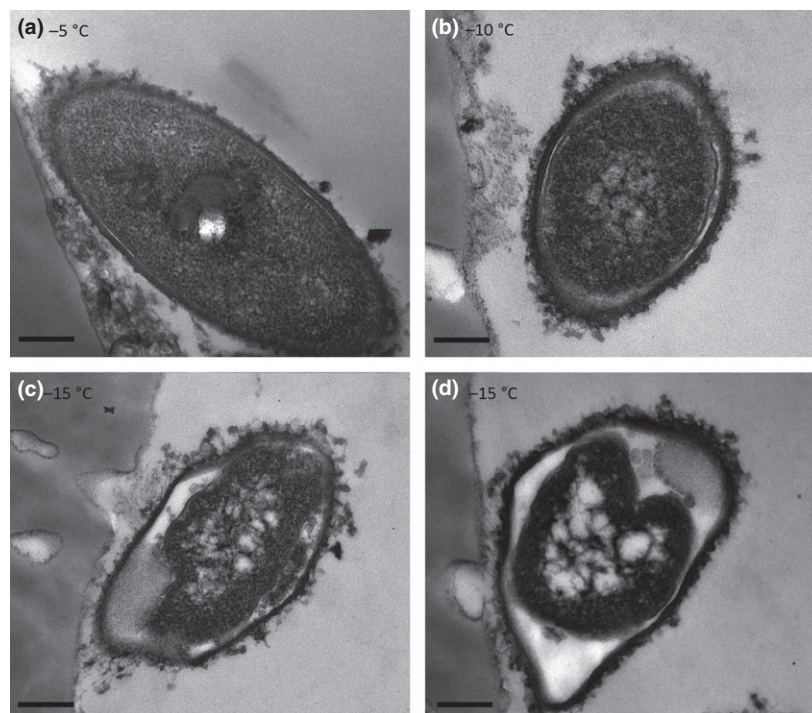


**Fig. 9.** Accumulation of polysaccharide granules in the cytoplasm of *Clostridium psychrophilum* at subzero temperatures,  $-5$  °C (a),  $-10$  °C (b) and  $-15$  °C (c, d) observed with TEM. Granules of polysaccharide storage material appear as electron translucent inclusions in the cytoplasm and accumulate in larger quantity at the lowest temperatures (c, d). Also visible are plasmolysis areas caused by extracellular freezing (c, d). Scale bar represents 200 nm.



## References

- Abboud R, Popa R, Souza-Egipsy V, Giometti CS, Tollaksen S, Mosher JJ, Findlay RH & Nealson KH (2005) Low-temperature growth of *Shewanella oneidensis* MR-1. *Appl Environ Microbiol* **71**: 811–816.
- Allen MA, Lauro FM, Williams TJ et al. (2009) The genome sequence of the psychrophilic archaeon, *Methanococcoides burtonii*: the role of genome evolution in cold adaptation. *ISME J* **3**: 1012–1035.
- Ayala-del-Río HL, Chain PS, Grzymalski JJ et al. (2010) The genome sequence of *Psychrobacter arcticus* 273-4, a psychroactive Siberian permafrost bacterium, reveals mechanisms for adaptation to low-temperature growth. *Appl Environ Microbiol* **76**: 2304–2312.
- Bakermans C (2008) Limits for microbial life at subzero temperatures. *Psychrophiles: From Biodiversity to Biotechnology* (Margesin R, Schinner F, Marx J-C & Gerday C, eds), pp. 17–28. Springer-Verlag, Berlin, Heidelberg.
- Bakermans C, Tsapin AI, Souza-Egipsy V, Gilichinsky DA & Nealson KH (2003) Reproduction and metabolism at  $-10^{\circ}\text{C}$  of bacteria isolated from Siberian permafrost. *Environ Microbiol* **5**: 321–326.
- Bakermans C, Tollaksen SL, Giometti CS, Wilkerson C, Tiedje JM & Thomashow MF (2007) Proteomic analysis of *Psychrobacter cryohalolentis* K5 during growth at subzero temperatures. *Extremophiles* **11**: 343–354.
- Baldwin WW & Bankston PW (1988) Measurement of live bacteria by Normarski interference microscopy and stereologic methods as tested with macroscopic rod-shaped models. *Appl Environ Microbiol* **54**: 105–109.
- Bergholz PW, Bakermans C & Tiedje JM (2009) *Psychrobacter arcticus* 273-4 uses resource efficiency and molecular motion adaptations for subzero temperature growth. *J Bacteriol* **191**: 2340–2352.
- Brambilla E, Hippe H, Hagelstein A, Tindall BJ & Stackebrandt E (2001) 16S rDNA diversity of cultured and uncultured prokaryotes of a mat sample from Lake Fryxell, McMurdo Dry Valleys, Antarctica. *Extremophiles* **5**: 23–33.
- Brook I (1986) Encapsulated anaerobic bacteria in synergistic infections. *Microbiol Rev* **50**: 452–457.
- Burke C, Liu M, Britton W, Triccas JA, Thomas T, Smith AL, Allen S, Salomon R & Harry E (2013) Harnessing single cell sorting to identify cell division genes and regulators in bacteria. *PLoS ONE* **8**: e60964.
- Casanueva A, Tuffin M, Cary C & Cowan DA (2010) Molecular adaptations to psychrophily: the impact of ‘omic’ technologies. *Trends Microbiol* **18**: 374–381.
- Clarke S, Mielke RE, Neal A, Holden P & Nadeau JL (2010) Bacterial and mineral elements in an arctic biofilm: a correlative study using fluorescence and electron microscopy. *Microsc Microanal* **16**: 153–165.
- Collins RE & Deming JW (2013) An inter-order horizontal gene transfer event enables the catabolism of compatible solutes by *Colwellia psychrerythraea* 34H. *Extremophiles* **17**: 601–610.
- Crabbé A, Leroy B, Wattiez R, Aertsen A, Leys N, Cornelis P & Van Houdt R (2012) Differential proteomics and physiology of *Pseudomonas putida* KT2440 under filament-inducing conditions. *BMC Microbiol* **12**: 282–291.
- Das T, Sharma PK, Busscher HJ, van der Mei HC & Krom BP (2010) Role of extracellular DNA in initial bacterial adhesion and surface aggregation. *Appl Environ Microbiol* **76**: 3405–3408.
- Davey HM & Hexley P (2011) Red but not dead? Membranes of stressed *Saccharomyces cerevisiae* are permeable to propidium iodide. *Environ Microbiol* **13**: 163–171.
- de Jong AE, Rombouts FM & Beumer RR (2004) Behaviour of *Clostridium perfringens* at low temperatures. *Int J Food Microbiol* **97**: 71–80.
- Deatherage BL & Cookson BT (2012) Membrane vesicle release in bacteria, eukaryotes, and archaea: a conserved yet underappreciated aspect of microbial life. *Infect Immun* **80**: 1948–1957.
- DeMaere MZ, Williams TJ, Allen MA et al. (2013) High level of intergenera gene exchange shapes the evolution of haloarchaea in an isolated Antarctic lake. *P Natl Acad Sci USA* **110**: 16939–16944.
- Flemming HC & Wingender J (2010) The biofilm matrix. *Nat Rev Microbiol* **8**: 623–633.
- Fonseca F, Marin M & Morris GJ (2006) Stabilization of frozen *Lactobacillus delbrueckii* subsp. *bulgaricus* in glycerol suspensions: freezing kinetics and storage temperature effects. *Appl Environ Microbiol* **72**: 6474–6482.
- Frias A, Manresa A, de Oliveira E, López-Iglesias C & Mercade E (2010) Membrane vesicles: a common feature in the extracellular matter of cold-adapted Antarctic bacteria. *Microb Ecol* **59**: 476–486.
- Gaudin M, Gauliard E, Schouten S, Houel-Renault L, Lenormand P, Marguet E & Forterre P (2013) Hyperthermophilic archaea produce membrane vesicles that can transfer DNA. *Environ Microbiol Rep* **5**: 109–116.
- Gloag ES, Turnbull L, Huang A et al. (2013) Self-organization of bacterial biofilms is facilitated by extracellular DNA. *P Natl Acad Sci USA* **110**: 11541–11546.
- Groudieva T, Grote R & Antranikian G (2003) *Psychromonas arctica* sp. nov., a novel psychrotolerant, biofilm-forming bacterium isolated from Spitzbergen. *Int J Syst Evol Microbiol* **53**: 539–545.
- Hammerschmidt S, Wolff S, Hocke A, Rosseau S, Müller E & Rohde M (2005) Illustration of pneumococcal polysaccharide capsule during adherence and invasion of epithelial cells. *Infect Immun* **73**: 4653–4667.
- Hinsa-Leasure SM, Koid C, Tiedje JM & Schultzehaus JN (2013) Biofilm formation by *Psychrobacter arcticus* and the role of a large adhesin in attachment to surfaces. *Appl Environ Microbiol* **79**: 3967–3973.
- Jeon CO, Park W, Ghiorse WC & Madsen EL (2004) *Polaromonas naphthalenivorans* sp. nov., a naphthalene-degrading bacterium from

- naphthalene-contaminated sediment. *Int J Syst Evol Microbiol* **54**: 93–97.
- Jones TH, Murray A, Johns M, Gill CO & McMullen LM (2006) Differential expression of proteins in cold-adapted log-phase cultures of *Escherichia coli* incubated at 8, 6 or 2°C. *Int J Food Microbiol* **107**: 12–19.
- Jones TH, Vail KM & McMullen LM (2013) Filament formation by foodborne bacteria under sublethal stress. *Int J Food Microbiol* **165**: 97–110.
- Justice SS, Hunstad DA, Cegelski L & Hultgren SJ (2008) Morphological plasticity as a bacterial survival strategy. *Nat Rev Microbiol* **6**: 162–168.
- Krembs C & Deming JW (2008) The role of exopolymers in microbial adaptation to sea ice. *Psychrophiles: From Biodiversity to Biotechnology* (Margesin R, Schinner F, Marx J-C & Gerday C, eds), pp. 247–264. Springer-Verlag, Berlin, Heidelberg.
- Krembs C, Eicken H & Deming JW (2011) Exopolymer alteration of physical properties of sea ice and implications for ice habitability and biogeochemistry in a warmer Arctic. *P Natl Acad Sci USA* **108**: 3653–3658.
- Kulp A & Kuehn MJ (2010) Biological functions and biogenesis of secreted bacterial outer membrane vesicles. *Annu Rev Microbiol* **64**: 163–184.
- Kuppusami S, Clokie MRJ, Panayi T, Ellis AM & Monks PS (2014) Metabolite profiling of *Clostridium difficile* ribotypes using small molecular weight volatile organic compounds. *Metabolomics*, DOI: 10.1007/s11306-014-0692-4 [Epub ahead of print].
- Li T, Wu TD, Mazéas L, Toffin L, Guerin-Kern JL, Leblon G & Bouchez T (2008) Simultaneous analysis of microbial identity and function using NanoSIMS. *Environ Microbiol* **10**: 580–588.
- Marchant R, Banat IM, Rahman TJ & Berzano M (2002) The frequency and characteristics of highly thermophilic bacteria in cool soil environments. *Environ Microbiol* **4**: 595–602.
- Margesin R & Miteva V (2011) Diversity and ecology of psychrophilic microorganisms. *Res Microbiol* **162**: 346–361.
- Matias VR & Beveridge TJ (2005) Cryo-electron microscopy reveals native polymeric cell wall structure in *Bacillus subtilis* 168 and the existence of a periplasmic space. *Mol Microbiol* **56**: 240–251.
- Mazur P (1984) Freezing of living cells: mechanisms and implications. *Am J Physiol* **247**: C125–C142.
- Meiners K, Krembs C & Gradinger R (2008) Exopolymer particles: microbial hotspots of enhanced bacterial activity in Arctic fast ice (Chukchi Sea). *Aquat Microb Ecol* **52**: 195–207.
- Méthé BA, Nelson KE, Deming JW *et al.* (2005) The psychrophilic lifestyle as revealed by the genome sequence of *Colwellia psychrerythraea* 34H through genomic and proteomic analyses. *P Natl Acad Sci USA* **102**: 10913–10918.
- Müller S & Nebe-von-Caron G (2010) Functional single-cell analyses: flow cytometry and cell sorting of microbial populations and communities. *FEMS Microbiol Rev* **34**: 554–587.
- Musat N, Halm H, Winterholler B, Hoppe P, Peduzzi S, Hillion F, Horreard F, Amann R, Jørgensen BB & Kuypers MM (2008) A single-cell view on the ecophysiology of anaerobic phototrophic bacteria. *P Natl Acad Sci USA* **105**: 17861–17866.
- Musat N, Foster R, Vagner T, Adam B & Kuypers MM (2012) Detecting metabolic activities in single cells, with emphasis on nanoSIMS. *FEMS Microbiol Rev* **36**: 486–511.
- Mykytczuk NC, Foote SJ, Omelon CR, Southam G, Greer CW & Whyte LG (2013) Bacterial growth at –15°C; molecular insights from the permafrost bacterium *Planococcus halocryophilus* Or1. *ISME J* **7**: 1211–1226.
- Niederberger TD, Perreault NN, Lawrence JR, Nadeau JL, Mielke RE, Greer CW, Andersen DT & Whyte LG (2009) Novel sulfur-oxidizing streamers thriving in perennial cold saline springs of the Canadian high Arctic. *Environ Microbiol* **11**: 616–629.
- Patel A, Noble RT, Steele JA, Schwalbach MS, Hewson I & Fuhrman JA (2007) Virus and prokaryote enumeration from planktonic aquatic environments by epifluorescence microscopy with SYBR Green I. *Nat Protoc* **2**: 269–276.
- Pecheritsyna SA, Arkhipova OV, Suzina NE, Lysanskaya VY, Laurinavichyus KS & Shcherbakova VA (2011) Intracellular polysaccharide of an anaerobic psychrophile *Clostridium algariphilum*. *Microbiology* **80**: 37–42.
- Pett-Ridge J & Weber PK (2012) NanoSIP: NanoSIMS applications for microbial biology. *Methods Mol Biol* **881**: 375–408.
- Polerecky L, Adam B, Milucka J, Musat N, Vagner T & Kuypers MM (2012) Look@NanoSIMS – a tool for the analysis of nanoSIMS data in environmental microbiology. *Environ Microbiol* **14**: 1009–1023.
- Riley M, Staley JT, Danchin A, Wang TZ, Brettin TS, Hauser LJ, Land ML & Thompson LS (2008) Genomics of an extreme psychrophile, *Psychromonas ingrahamii*. *BMC Genom* **9**: 209–228.
- Rodrigues DF & Tiedje JM (2008) Coping with our cold planet. *Appl Environ Microbiol* **74**: 1677–1686.
- Rodrigues DF, Ivanova N, He Z, Huebner M, Zhou J & Tiedje JM (2008) Architecture of thermal adaptation in an *Exiguobacterium sibiricum* strain isolated from 3 million year old permafrost: a genome and transcriptome approach. *BMC Genom* **9**: 546–563.
- Schwarz H & Koch AL (1995) Phase and electron microscopic observations of osmotically induced wrinkling and the role of endocytotic vesicles in the plasmolysis of the Gram-negative cell wall. *Microbiology* **141**: 3161–3170.
- Soina VS, Vorobiova EA, Zvyagintsev DG & Gilichinsky DA (1995) Preservation of cell structures in permafrost: a model for exobiology. *Adv Space Res* **15**: 237–242.
- Spring S, Merkhoffer B, Weiss N, Kroppenstedt RM, Hippe H & Stackebrandt E (2003) Characterization of novel psychrophilic clostridia from an Antarctic microbial mat: description of *Clostridium frigidum* sp. nov., *Clostridium lacusfrigidum* sp. nov., *Clostridium bowmanii* sp. nov. and

- Clostridium psychrophilum* sp. nov. and reclassification of *Clostridium laramiense* as *Clostridium estertheticum* subsp. *laramiense* subsp. nov. *Int J Syst Evol Microbiol* **53**: 1019–1029.
- Suo Z, Avci R, Deliorman M, Yang X & Pascual DW (2009) Bacteria survive multiple puncturings of their cell walls. *Langmuir* **25**: 4588–4594.
- Swanson JA (2013) The noodle defense. *J Cell Biol* **203**: 871–873.
- Wagner M (2008) Single-cell ecophysiology of microbes as revealed by Raman microspectroscopy or secondary ion mass spectrometry imaging. *Annu Rev Microbiol* **63**: 411–429.
- Yoon MY, Lee KM, Park Y & Yoon SS (2011) Contribution of cell elongation to the biofilm formation of *Pseudomonas aeruginosa* during anaerobic respiration. *PLoS ONE* **6**: e16105.
- Young KD (2006) The selective value of bacterial shape. *Microbiol Mol Biol Rev* **70**: 660–703.

## Supporting Information

Additional Supporting Information may be found in the online version of this article:

**Fig. S1.** Cell morphology changes in *C. psychrophilum* in response to temperatures.

**Fig. S2.** Comparison between conventional glutaraldehyde-formaldehyde fixation (a) and lysine-acetate ruthenium red (LRR) (b) for the visualisation of bacterial cell surface and capsular material.